Available online at www.sciencedirect.com
ScienceDirect
Polymer 48 (2007) 3694–3702
polymer
www.elsevier.com/locate/polymer

Amphiphilic macromolecular nanostructure materials derived from 5-(octanoate methyl)bicyclo[2.2.1]hept-2-ene and 5-(phthalimide methyl)bicyclo[2.2.1]hept-2-ene via ring-opening metathesis copolymerization

Der-Jang Liaw [a,*], Kun-Li Wang [b], Tsang-Pin Chen [a], Kueir-Rarn Lee [c], Juin-Yih Lai [c]

[a] *Department of Chemical Engineering, National Taiwan University of Science and Technology, 106 Taipei, Taiwan*
[b] *Department of Chemical Engineering and Biotechnology, National Taipei University of Technology, 106 Taipei, Taiwan*
[c] *R&D Center for Membrane Technology, Chung-Yuan Christian University, 32023 Chung Li, Taiwan*

Received 14 November 2006; received in revised form 16 April 2007; accepted 18 April 2007
Available online 24 April 2007

Abstract

Novel highly stable polynorbornenes with self-assembling amphiphilic architecture containing hydrophilic ammonium salt and hydrophobic alkyl ester group were obtained via ring-opening metathesis polymerization (ROMP) of 5-(octanoate methyl)bicyclo[2.2.1]hept-2-ene (NBMO) and 5-(phthalimide methyl)bicyclo[2.2.1]hept-2-ene (NBMPI), hydrogenation, hydrazinolysis, and subsequent quaternization. Polymeric micelles of such amphiphilic random and block polynorbornenes formed in solvents by varying the content of ammonium salts were investigated. Amphiphilic block copolymers exhibited perfect spherical morphology. Nanoscale polymeric micelles of random copolymers with 50–75 mol% of ammonium salts were roughly spherical in shape, while the morphologies of micelles transferred into network-like aggregates as hydrophilic contents of the random copolymers are higher than 80 mol%. The formation and fine structures of micelles were investigated by dynamic light scattering (DLS), TEM, and fluorescence technique using pyrene as fluorescence probe.

Keywords: Nanosphere; Micelles; ROMP

1. Introduction

At the forefront of nanotechnology is the on-going quest to develop easily accessible reaction and templating media, which offer compositional and/or architectural control on a nanometer scale [1]. Over the past few years, polymers containing hydrophilic and hydrophobic components have gained the interest from both theoretical and synthetic point of view [1]. The tendency of the hydrophobic parts to aggregate into micelles in water and also the surface active properties exhibited by such amphiphilic polymers are two features that have been thoroughly investigated and exploited in miscellaneous applications [1]. In addition to compartmentalization of hydrophobic drugs, the amphiphilic macromolecules must meet further criteria to be effective drug carriers. Biocompatibility, appropriate size (10–100 nm) for blood circulation, and a low critical micelle concentration (CMC) are important characteristics that lead to improved bioavailability, reduction of toxicity, enhanced permeability across physiological barriers, and substantial changes in drug biodistribution [2–7]. For many years, quaternary ammonium salt (QAS) has been applied as disinfectants [8] due to its antimicrobial activities and other applications such as surfactants [9], transfer agents [10], etc. Quaternized cationic polymers can exhibit higher activities than the corresponding low molecular weight model compound [11]. With a comprehensive understanding of their chemical compositions and corresponding relationship to

* Corresponding author. Tel.: +886 2 2737 6638/2733 5050; fax: +886 2 2378 1441/2737 6644.
E-mail addresses: liaw@ch.ntust.edu.tw, liaw6565@yahoo.com.tw (D.-J. Liaw).

0032-3861/$ - see front matter © 2007 Elsevier Ltd. All rights reserved.
doi:10.1016/j.polymer.2007.04.034

physical properties, amphiphilic macromolecules can be designed for optimal drug delivery.

In our previous papers [12–16], we reported about the synthesis and characterization of random and block copolynorbornenes with various side chains via ROMP. In present approach, various random and block copolymers with varying composition of 5-(octanoate methyl)bicyclo[2.2.1]hept-2-ene (NBMO) and 5-(phthalimide methyl)bicyclo[2.2.1]hept-2-ene (NBMPI) were synthesized to investigate the formation, structure, and morphologies of the polymeric micelles. The association of polymer molecules in solvents will be confirmed by fluorescence spectroscopy. The size and morphologies of aggregates will be characterized by transmission electron microscopy (TEM).

2. Experimental

2.1. Materials

Octanoyl chloride, allyl alcohol, allyl amine, phthalic anhydride and *p*-toluenesulfonhydrazide were purchased from Acros, Belgium. Benzylidene bis(tricyclohexylphosphine)dichlororuthenium $\{Cl_2Ru(CHPh)[P(C_6H_{11})_3]_2\}$ was purchased from Aldrich, USA. Synthesis of 5-(hydroxy methyl)bicyclo[2.2.1]hept-2-ene (NBMOH) (b.p. = 93–95 °C/13 mmHg) and 5-(amino methyl)bicyclo[2.2.1]hept-2-ene (NBMA) (b.p. = 60–61 °C/11 mmHg) was accomplished via the Diels–Alder condensation of freshly cracked cyclopentadiene with allyl alcohol and allyl amine, respectively.

2.2. Synthesis of 5-(octanoate methyl)bicyclo[2.2.1]hept-2-ene (NBMO)

Ester derivative of norbornene such as 5-(octanoate methyl)-bicyclo[2.2.1]hept-2-ene (NBMO) was prepared as described in previous literatures [12–14].

2.3. Preparation, hydrogenation, hydrazinolysis and quaternization of random poly(NBMO-r-NBMPI)s via ring-opening metathesis polymerization

The monomer, NBMPI was prepared by azeotropic removal of water from an equimolar solution of 5-(amino methyl)-bicyclo[2.2.1]hept-2-ene (NBMA) and phthalic anhydride in xylene as previously reported, m.p. = 99–100 °C [15]. Random copolymers, poly(NBMPI-*r*-NBMO)s were obtained by ROMP using Ru-catalyst from different ratios of NBMO and NBMPI. Hydrogenation of random poly(NBMPI-*r*-NBMPO)s was carried out by using *p*-toluenesulfonhydrazide as a hydrogenating agent, which was described in the previous paper [16]. Random copolymers (0.2 g, 0.8 mmol) were suspended in 15 mL of ethanol in an Schlenk tube, to which 5 mL of hydrazine monohydrate was added. The mixture was degassed thrice via a freeze–pump–thaw cycle, then the tube was heated to 100 °C for 12 h for hydrazinolysis. The quaternization was subsequently carried out by using $HCl_{(g)}$ at room temperature for 2 h. The quaternized copolymer was dissolved in water, filtered and then precipitated from acetone. The detailed procedures were reported in our previous paper [16].

2.4. Preparation, hydrogenation, hydrazinolysis and quaternization of block poly(NBMPI-b-NBMO)s via living ring-opening metathesis polymerization

Block copolymers synthesized from monomers, NBMPI and NBMO, were obtained by ROMP using Ru-catalyst in different molar ratios of NBMPI and NBMO. As an example, poly($NBMPI_{100}$-*b*-$NBMO_{100}$) with molar ratio 1/1 of [NBMPI]/[NBMO] ($f_{NBMQ(th)} = 50$ mol%) is described as follows. The monomer (1.54 g, 6.08 mmol) ([NBMPI]/[catalyst] = 100), NBMPI was dissolved in 10 mL of anhydrous methylene chloride and then degassed via a freeze–pump–thaw cycle. After complete degassing, the catalyst solution [50 mg of Ru-catalyst (6.08×10^{-2} mmol) in 0.5 mL of anhydrous methylene chloride] was injected into the monomer solution by a syringe. The pink solution was vigorously stirred at ambient temperature for 1 h. Prepolymer [poly(NBMPI)] with $\overline{M}_n = 2.25 \times 10^4$ and PDI = 1.8 was determined using gel permeation chromatography (GPC). Additional monomer solution of NBMO (1.52 g, 6.08 mmol) ([NBMO]/[catalyst] = 100) in methylene chloride was injected into the still-living reaction mixture and the solution was stirred for another 2 h at 30 °C. The reaction was terminated by the addition of a small amount of ethyl vinyl ether. After termination, the solution was stirred for an additional 5 min, and the block copolymer was precipitated in excess of methanol and the white polymer was further purified by dissolving in methylene chloride and reprecipitating in methanol. The block copolymer was dissolved in benzene, frozen, and dried. Hydrogenation, hydrazinolysis and quaternization were carried out in the same procedures as described for random copolymers.

2.5. Preparation of TEM samples

The polymer solutions of 0.2 g dL^{-1} (soluble in ethanol/dichloromethane = 2/1, v/v) or 0.02 g dL^{-1} (soluble in ethanol) were sonicated for 15 min at room temperature. The copper grids coated with a thin carbon film were treated with a drop of 5 μL solution and the solvent was evaporated under vacuum at room temperature.

2.6. Sample preparations for DLS and fluorescence measurements

To a saturated solution of pyrene (ca. 2 μM), trace amount of polymer was added. Various concentrations of polymer solution were sonicated for 15 min at room temperature. The samples were kept at room temperature overnight before DLS or fluorescence measurement.

2.7. Measurements

IR spectra were recorded in the range 4000–500 cm^{-1} for the synthesized monomers and polymers on KBr disks

(Bio-Rad FTS-3500 spectrometer). NMR spectra were recorded by using Bruker Avance 500 NMR (^{1}H at 500 MHz and ^{13}C at 125 MHz). The weight-average ($\overline{M}_w$) and number-average molecular weights ($\overline{M}_n$) were determined by gel permeation chromatography (GPC). Four Waters (Ultrastyragel) columns 300 × 7.7 mm (guard, 10^5, 10^4, 10^3, 500 Å in a series) were used for GPC analysis with tetrahydrofuran (THF) (1 mL min^{-1}) as the eluent. The eluents were monitored with a refractive index (RI) detector (Schambeck SFD GmbH, RI 2000). Polystyrene was used as the standard. Electron micrographs were recorded with a JEOL JSM-6500 scanning electron microscope (SEM) at 20 kV and HITACHI H-7100 transmission electron microscope (TEM) at 150 kV. The hydrodynamic radius of polymer in solution was measured by dynamic light scattering (Photal, DLS-7000) and the formation of micelles by fluorescence spectra, which were recorded by a spectrophotometer (Shimadzu, RF-5031).

3. Results and discussion

3.1. Characterization of various random copolymers and block copolymers

The preparation and characterization (^{1}H NMR, ^{13}C NMR, H–H COSY, and C–H COSY) of monomers, NBMPI and NBMO, were reported in our previous papers [15,16]. Random copolymers poly(NBMPI-*r*-NBMO)s of NBMPI and NBMO in various ratios were polymerized via ROMP using Ru-catalyst as outlined in Scheme 1. The molar fractions of NBMPI ($f_{NBMPI(exp)}$) in random poly(NBMPI-*r*-NBMO)s were estimated from the relative peak area of phthalic aromatic proton resonances and olefinic proton resonances. The results are summarized in Table 1. Hydrogenation was carried out using *p*-toluenesulfonhydrazide as hydrogenating agent, to get hydrogenated polymers poly(HNBMPI-*r*-HNBMO)s. From the ^{1}H NMR spectra, disappearance of the unsaturated double bond between 5.2 and 5.6 ppm clearly reveals the successes of hydrogenation. Subsequent hydrazinolysis was carried out with hydrazine in ethanol to change phthalic imide into amino group, and then quaternization by adding $HCl_{(g)}$ was proceeded at room temperature to form hydrophilic ammonium salt group at the pendant, which results in the formation of poly(HNBMQ-*r*-HNBMO)s.

The living ROMP characteristic of NBMPI was demonstrated in our previous paper [15]. Herein we applied the living characteristic to prepare block poly(NBMPI-*b*-NBMO)s by adding a second monomer, NBMO, to the unterminated poly(NBMPI) reaction mixture. Based on the molecular weight of poly(NBMPI) and block poly(NBMPI-*b*-NBMO) measured from GPC, the segments of poly(NBMPI) and poly(NBMO) in block poly(NBMPI-*b*-NBMO) and molar fraction of NBMPI ($f_{NBMPI(exp)}$) can be calculated. For the block poly(NBMPI$_{100}$-*b*-NBMO$_{100}$), the yield of the polymer was 85%. Composition of block poly(NBMPI$_{100}$-*b*-NBMO$_{100}$) was calculated by GPC and found to be about 90 of poly(NBMPI) segment and 86 of poly(NBMO) segment ($f_{NBMPI(exp)}$ = 51 mol%, $(\overline{M}_n) = 4.41 \times 10^4$, PDI = 1.3). The result of gel permeation chromatograph as shown in Fig. 1 shows the shift of molecular weight curves in GPC after block copolymerization via ROMP due to second block polymer poly(NBMO). In ^{1}H NMR, the aromatic phthalimide proton resonances appeared between δ (ppm) 7.6 and 7.8. The unsaturation double bond proton resonance in the polymer main chain for block poly(NBMPI$_{100}$-*b*-NBMO$_{100}$) appeared between δ (ppm) 5.2 and 5.6. The molar fraction of NBMPI in block poly(NBMPI$_{100}$-*b*-NBMO$_{100}$) estimated from the relative peak

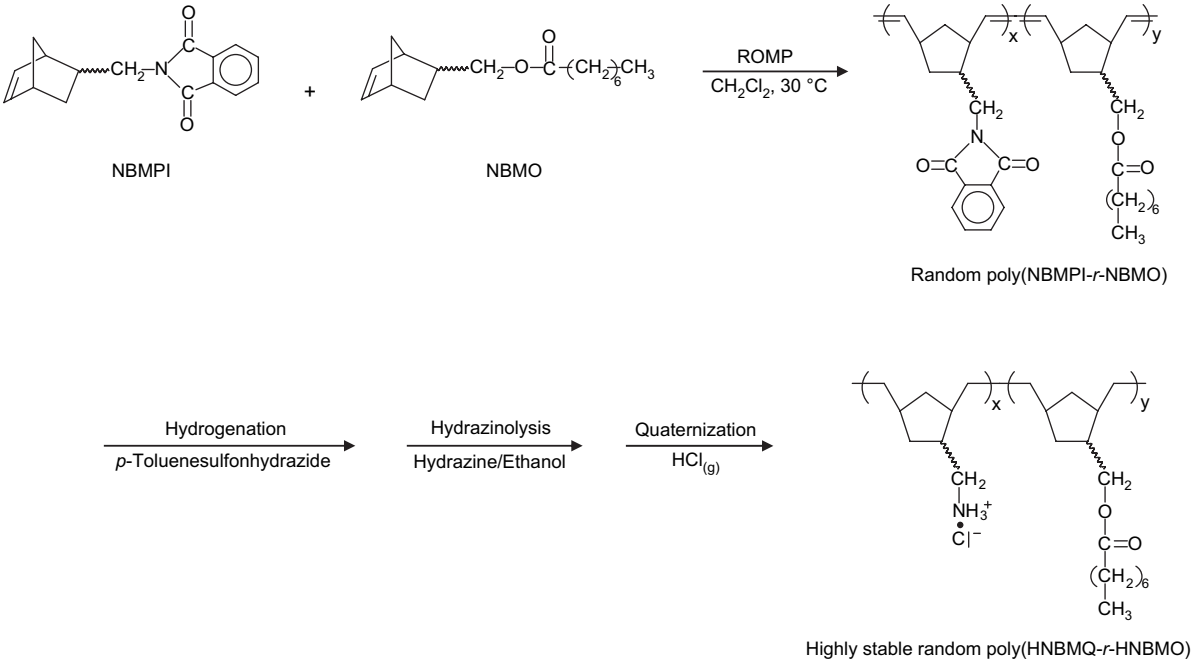

Scheme 1. Preparation of highly stable random poly(HNBMQ-*r*-HNBMO)s.

Table 1
Composition, micellar characterization and particle size of random poly(HNBMQ-*r*-HNBMO)s

Polymer code	Content of ammonium salt		$M_n \times 10^{-5}$ [c] (calcd)	$M_n \times 10^{-5}$ [c]	PDI[c]	CAC $\times 10^4$ [d] ($g\,dL^{-1}$)	CMC[d] ($g\,dL^{-1}$)	D_{TEM}[d] (nm)
	($f_{HNBMQ(th)}$)[a] (mol%)	($f_{HNBMQ(ex)}$)[b] (mol%)						
Poly($HNBMQ_{250}$-*r*-$HNBMO_{250}$)	50	48.7	1.26	0.83	1.5	–[e]	–[e]	5.0
Poly($HNBMQ_{500}$-*r*-$HNBMO_{250}$)	67	67.2	1.89	1.42	2.9	5.6	0.1	5.5
Poly($HNBMQ_{750}$-*r*-$HNBMO_{250}$)	75	74.9	2.52	1.98	4.9	32	0.3	13.7
Poly($HNBMQ_{1000}$-*r*-$HNBMO_{250}$)	80	76.6	3.15	2.17	6.1	79	–[f]	–[g]
Poly($HNBMQ_{1000}$-*r*-$HNBMO_{100}$)	91	91	2.77	1.66	2.5	400	–[f]	–[g]

[a] The definition of f_{HNBMQ}: the molar fraction of HNBMQ segment.
[b] The molar fractions were calculated from ^{1}H NMR of poly(NBMO-*r*-NBMPI)s.
[c] The molecular weights were calculated and determined by GPC in THF using polystyrene as standard for prepolymer poly(NBMPI-*r*-NBMO)s.
[d] CAC: critical aggregation concentration; CMC: critical micelle concentration; D_{TEM}: diameter of the particle detected from TEM.
[e] The polymer is insoluble in water.
[f] The CMC could not be detected.
[g] From TEM, the D_{TEM} could not be detected because of network-like structure.

areas of phthalic aromatic proton resonances and olefinic proton resonances is 56 mol%, which is higher than the value calculated from GPC. Poly(HNBMQ-*b*-HNBMO)s were prepared via subsequent hydrogenation, hydrazinolysis and quaternization of block poly(NBMPI-*b*-NBMO)s. The chemical structures of the synthetic intermediates were also verified by the same methods as described in the structure identifications of random poly(NBMPI-*r*-NBMO)s. The other block polymers were synthesized and verified in the same manner. The yield of poly($HNBMPI_{1000}$-*b*-$HNBMO_{100}$) was 82%. The mole fraction of NBMPI ($f_{NBMPI(exp)}$) was 92.7 mol% calculated from GPC and 91 mol% from ^{1}H NMR. The yield of quaternized block copolymer, poly($HNBMQ_{1000}$-*b*-$HNBMO_{100}$), was 80%. The results confirmed the formation of block polymers and the living ROMP nature of the monomer, NBMPI.

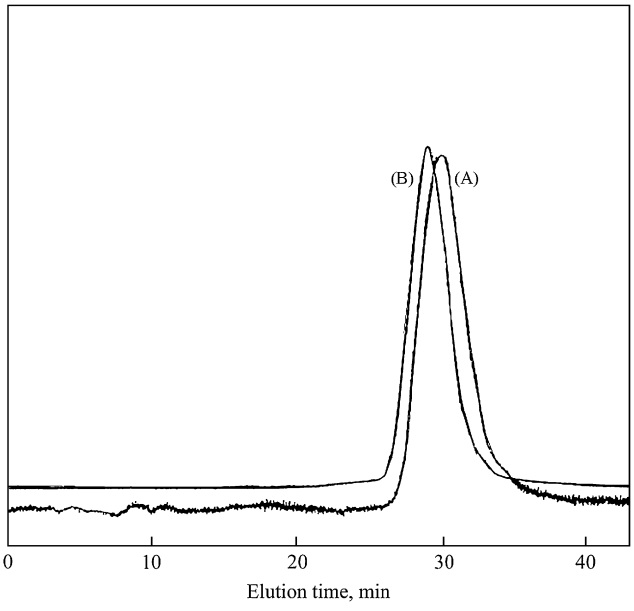

Fig. 1. GPC curves of (A) poly(NBMPI) (corresponding to the first block) and (B) a block copolymer poly($NBMPI_{100}$-*b*-$NBMO_{100}$) ($f_{HNBMQ(th)} = 50$ mol%). The molecular weights were determined relative to polystyrene (PS) standards.

3.2. Micelles observation of block polymers

DLS (dynamic light scattering) measurement of micelles in ethanol was performed and hydrodynamic radius was calculated as shown in Fig. 2. The hydrodynamic radius (R_h) of poly($HNBMQ_{100}$-*b*-$HNBMO_{100}$) ($f_{HNBMQ(th)} = 50$ mol%; $f_{HNBMQ(exp)} = 51$ mol% by GPC) in ethanol decreases as the concentration of poly($HNBMQ_{100}$-*b*-$HNBMO_{100}$) increases, and then reaches a steady value about 160 nm at 3.2×10^{-2} g dL^{-1}. In our previous study [13], the poly(HNBMO) was insoluble in ethanol. However, quaternized block copolymer poly($HNBMQ_{100}$-*b*-$HNBMO_{100}$) could be soluble in ethanol. Therefore, the difference of solubility resulted from the quaternized hydrophilic segments of polymer. In general, the polymer allows each segment to interact with its favored environment. The polymer can form aggregates in which the hydrophobic segments are oriented within the micelle and the hydrophilic segments are exposed to the solvent. If the size of micelles was controlled by the concentration of hydrophobic segments, larger size of micelles could be expected to form at higher concentration. However, the results

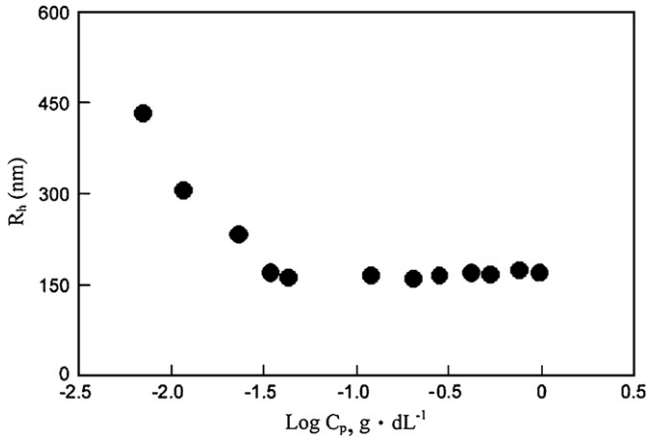

Fig. 2. Radius of hydrations of poly($HNBMQ_{100}$-*b*-$HNBMO_{100}$), $f_{HNBMQ} =$ 50 mol%, obtained from DLS measurement in ethanol at various polymer concentrations.

are contradictory from DLS measurement, in which the size of micelles keeps constant beyond concentration of 3.2×10^{-2} g dL^{-1}. Accordingly, the hydrodynamic radius of the cationic polymer in ethanol solution could result from electrostatic repulsive forces balance between intra- and inter-micelles [17]. As hydrophobic segments aggregate, the cations will be located at the surroundings of the micelles. When polymer concentration is increased, the repulsive electrostatic forces between micelles increase and then reduce the size of micelles resulted so that the repulsive forces within intra-micelles increase. Consequently, the size of micelles might reach a stable size due to the balance of electrostatic repulsive forces of intra- and inter-micelle. Fig. 3 shows the TEM micrographs of the micelles of poly(HNBMQ$_{100}$-*b*-HNBMO$_{100}$), which was prepared from a polymer ethanol solution at the concentration of 0.02 g dL^{-1}. The dark core regions correspond to hydrophobic segment of HNBMO in poly(HNBMQ$_{100}$-*b*-HNBMO$_{100}$). It can be seen from Fig. 3 that poly(HNBMQ$_{100}$-*b*-HNBMO$_{100}$) micelle is roughly spherical in shape. The average diameter of cores calculated from the TEM micrograph (Fig. 3) is ca. 224 nm (radius 112 nm). From the DLS result (Fig. 2), the hydrodynamic radius of poly(HNBMQ$_{100}$-*b*-HNBMO$_{100}$) in ethanol at 0.02 g dL^{-1} is 240 nm. The hydrodynamic diameter of micelles in ethanol solution measured by DLS is more than twice as large as the diameter calculated from TEM. This variation could be resulted from the influence of the solvent.

3.3. Micelles observation of random polymers

As shown in Fig. 4, it is interesting to find the individual micelles of random copolymers at concentration of 0.2 g dL^{-1} with composition range from 50 to 80 mol% ammonium salt (f_{HNBMQ}) in TEM micrographs as isolated nanometer-scale sphere, and their average diameters were calculated in the range of 5.0–13.7 nm from TEM micrographs. These results indicate that the intra-polymer aggregates formed by the random copolymer might be due to the formation of unimer (Fig. 4A–C) depending on the molar ratio of hydrophilic/hydrophobic group, i.e., the charge density of cation. When ammonium salt content (f_{HNBMQ}) was increased to 80 mol% ($f_{HNBMQ(exp)} = 76.6$ mol% by ^{1}H NMR), the micelle morphology changed from spherical to network-like aggregates (Fig. 4D), which is due to hydrophobically cross-linked chains of interpolymers.

From these results and observations of TEM micrographs and DLS, a conceptual illustration of self-assembly micelles for random poly(HNBMQ-*r*-HNBMO)s and block poly(HNBMQ-*b*-HNBMO)s is shown in Fig. 5.

The amount of hydrophobic segments is fixed (five repeating units in Fig. 5) and the amount of hydrophilic segments is drawn in different contents corresponding to the values of f_{HNBMQ}. For the random polymers, the polymer chains with low f_{HNBMQ} form unimers. If there is no electrostatic repulsive force in the polymer, the size of micelles will be the same due to the same hydrophobic amounts. However, from the TEM result, the size of micelles depended on the structures of amphiphilic polymers, which have the same hydrophobic content and different hydrophilic contents. Therefore, the size of the micelles will be affected by the electrostatic repulsive force of cations, which are attached on the polymer chains. For the same polymer concentration, the polymer with higher f_{HNBMQ} exhibits stronger intra-polymer repulsive force, resulting in the expansion of the size of micelles. The spherical morphologies of the micelles were observed in TEM (Fig. 4A–C). It might be due to the thermodynamic stability (Fig. 5A–C). Further, the intra-polymer electrostatic repulsive forces increase as the amount of hydrophilic segments with positive charge increases. The structure of unimers will be destroyed when the repulsive forces of intra-polymer are higher than the interaction force between hydrophobic segments. Instead of unimers, on the other hand, hydrophobically cross-linked

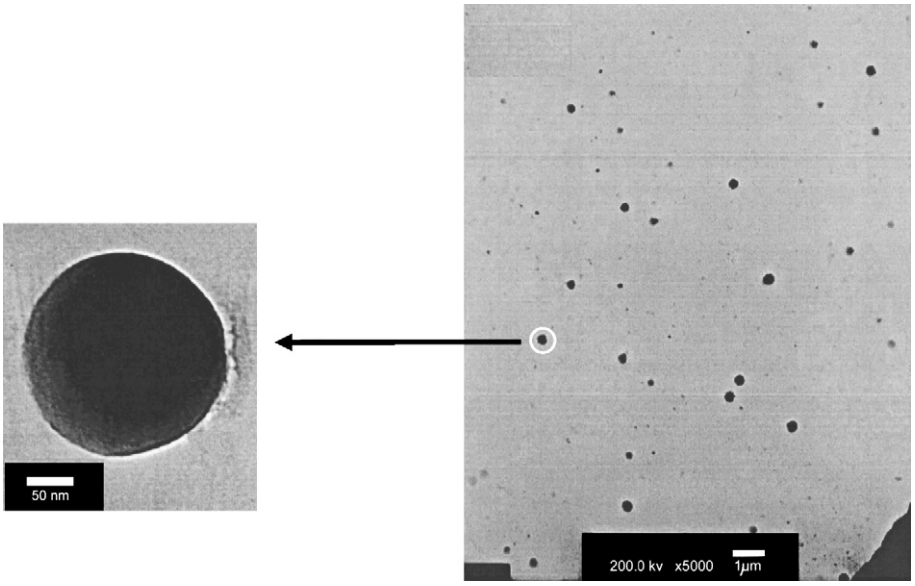

Fig. 3. TEM micrographs of poly(HNBMQ$_{100}$-*b*-HNBMO$_{100}$) prepared from ethanol solution.

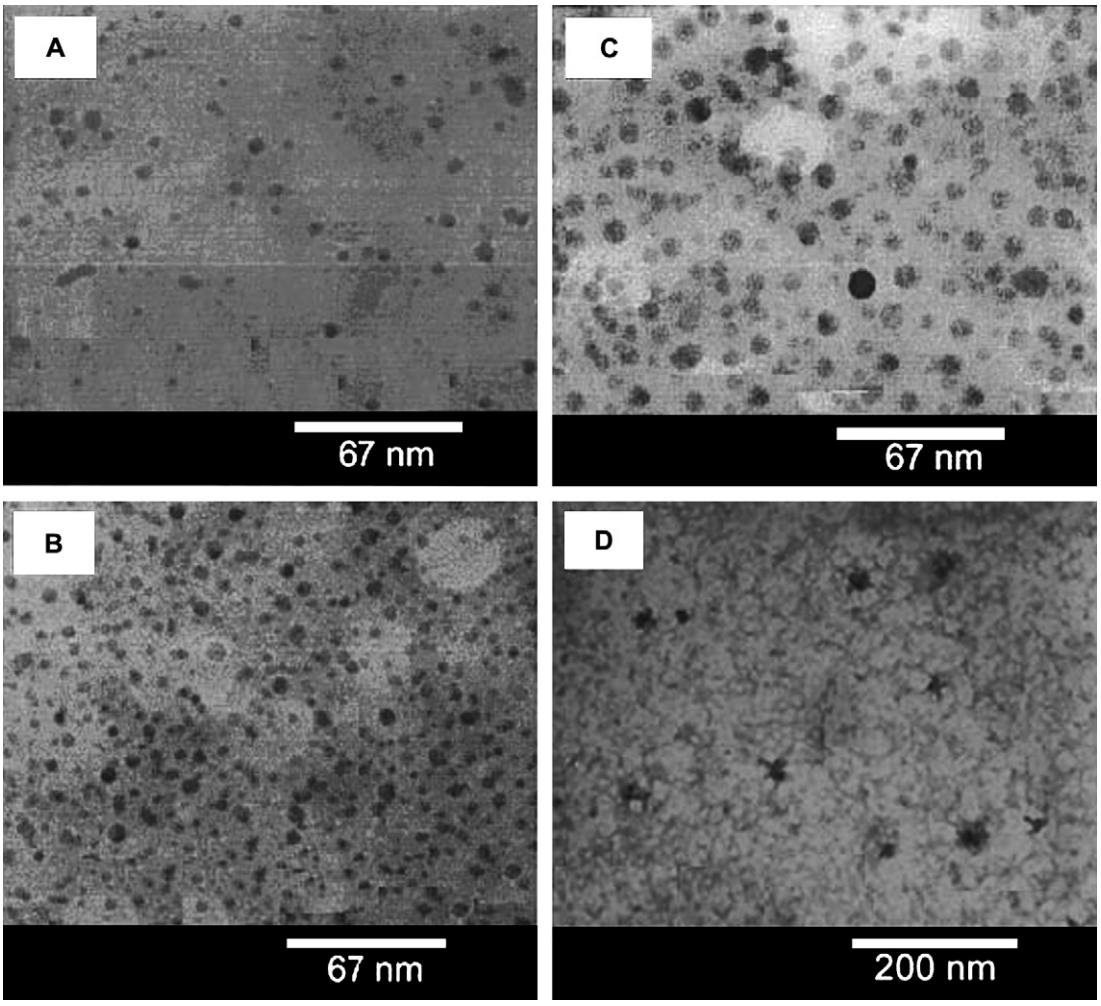

Fig. 4. TEM micrographs of various random poly(HNBMQ-*r*-HNBMO)s at concentration of 0.2 g dL^{-1}. The content of ammonium salt = (A) 50 mol% (poly($HNBMQ_{250}$-*r*-$HNBMO_{250}$)); (B) 67 mol% [poly($HNBMQ_{500}$-*r*-$HNBMO_{250}$)]; (C) 75 mol% [poly($HNBMQ_{750}$-*r*-$HNBMO_{250}$)]; (D) 80 mol% [poly-($HNBMQ_{1000}$-*r*-$HNBMO_{250}$)]. All prepared from ethanol/methylene chloride (2/1, v/v).

chains (network-like morphologies, Fig. 5D) were observed. This illustration is evidenced from the TEM observations (Fig. 4D). For the block copolymers (Fig. 5E), hydrophobic segments aggregate to form unicore multipolymer micelle having cationic segments located at outside of the micelle. As described previously in DLS results, the size of micelles was controlled by the electrostatic repulsive forces of intra- and inter-micelle. The result of DLS (Fig. 2) is also the evidence for supporting this conceptual illustration.

3.4. Hydrophobic microdomains of polymers formed by alkyl ester groups

Pyrene is one of the few condensed aromatic hydrocarbons, which shows significant fine structure (vibronic bands) in its monomer fluorescence spectra in solution phase. Hence, pyrene molecule is a useful fluorescence probe for characterization of molecular assemblies of numerous associating polymers [18]. Relative intensities of the vibronic bands of pyrene fluorescence are known to show a significant dependence on the microenvironmental polarity around pyrene; the relative intensity of the third to first vibrational peaks (I_3/I_1) in fluorescence spectra of pyrene reflects the polarity in local media where pyrene exists, i.e., I_3/I_1 ratio being larger in less polar media [18]. Therefore, the I_3/I_1 ratio can be used to discuss environmental effects on pyrene fluorescence. Furthermore, excimer emission was investigated by fluorescence measurement to elucidate the solution's behavior. Kramer reported that as the degree of hydrophobic association increases, interaction between isolated, covalently bound fluorescent hydrophobes allows the formation of dimeric, sandwich-like conformations that subsequently lead to excimer formation [19]. That is, excimer formation becomes more favorable as the distance between fluorescent pyrene molecules decreases. The emission ratio of I_E/I_M reflects intra-/interchain interactions of pyrene groups in polymer solution, where I_E/I_M is the ratio of intensities of excimer and monomer fluorescence [19,20].

To a saturation solution of pyrene (ca. 2 μM), trace amount of polymer was introduced. Fluorescence measurement was carried out for the dilute solutions (3.16×10^{-5}–3.16 g dL^{-1}). In Fig. 6, the I_3/I_1 ratios for all random copolymers are plotted against log(polymer concentration) [log C_p]

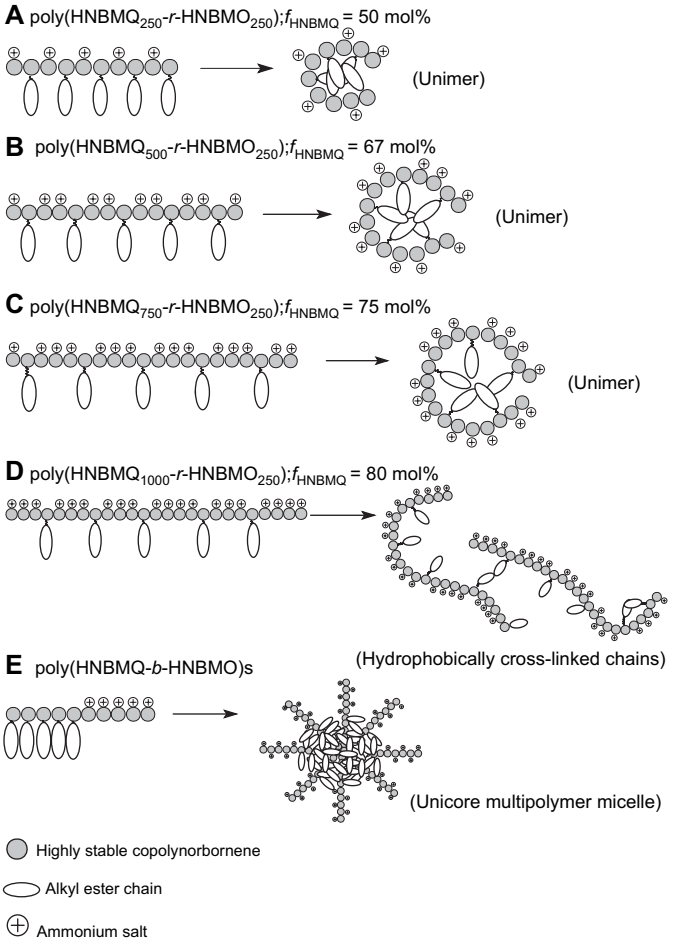

Fig. 5. Conceptual illustration of self-assembly micelles as a model for (A) random poly(HNBMQ$_{250}$-*r*-HNBMO$_{250}$) ($f_{HNBMQ} = 50$ mol%) (unimer), (B) random poly(HNBMQ$_{500}$-*r*-HNBMO$_{250}$) ($f_{HNBMQ} = 67$ mol%) (unimer), (C) random poly(HNBMQ$_{750}$-*r*-HNBMO$_{250}$) ($f_{HNBMQ} = 75$ mol%) (unimer), (D) random poly(HNBMQ$_{1000}$-*r*-HNBMO$_{250}$) ($f_{HNBMQ} = 80$ mol%) (hydrophobically cross-linked chains) and (E) block poly(HNBMQ-*b*-HNBMO)s (unicore multipolymer micelle).

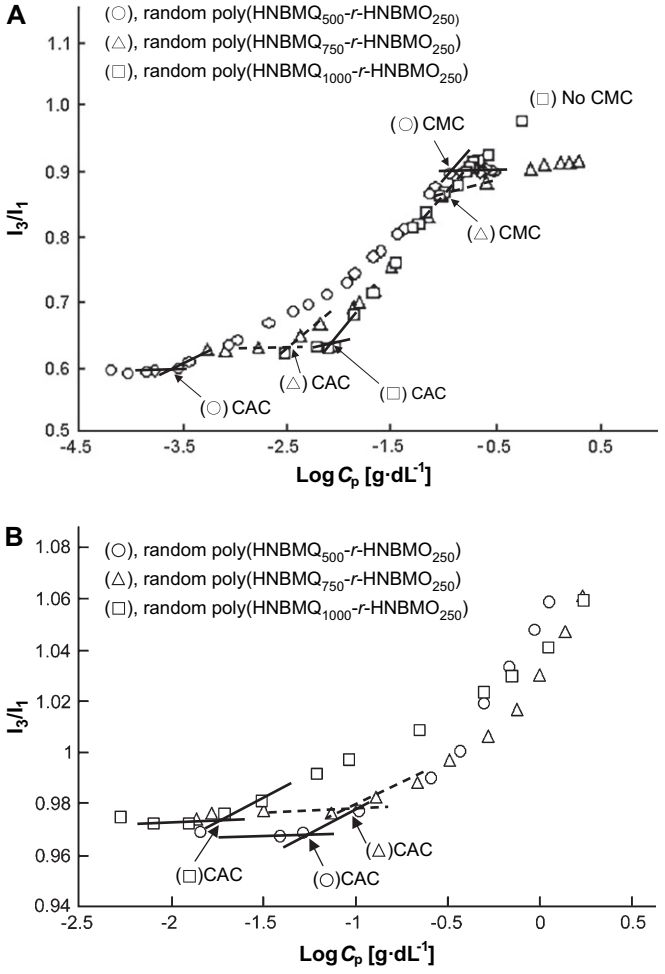

Fig. 6. Plots of log C_p *vs.* I_3/I_1 ratio for random poly(HNBMQ-*r*-HNBMO)s in (A) water and (B) cosolvent [ethanol:methylene chloride = 2:1 (v/v)]. The content of ammonium = 67 mol% (○), 75 mol% (△), and 80 mol% (□).

in water (Fig. 6A) and in cosolvent [ethanol/methylene chloride = 2/1 (v/v)] (Fig. 6B).

In the polymer aqueous, the I_3/I_1 ratios for all copolymers are around 0.6 at lower polymer concentration, which are practically the same as that for pyrene in water. This indicates that there is no formation of polymeric aggregates in aqueous solution [18]. As the polymer concentration is gradually increased, the I_3/I_1 ratio begins to increase significantly at a certain polymer concentration. Polymer with higher content of HNBMO (i.e., lower content of HNBMQ) exhibited higher influence on the ratio of intensity (I_3/I_1) of pyrene molecule. In the case of random poly(HNBMQ$_{500}$-*r*-HNBMO$_{250}$) ($f_{HNBMQ} = 67$ mol%), the I_3/I_1 ratio begins to increase at a polymer concentration (C_p) of 5.6×10^{-4} g dL^{-1}, which is defined as a critical aggregation concentration (CAC). As the polymer concentration is near 0.1 g dL^{-1}, the value of I_3/I_1 reached a constant value (ca. 0.9). The similar phenomena also appeared for other copolymers. From Fig. 6A, the CAC of random poly(HNBMQ$_{750}$-*r*-HNBMO$_{250}$) and random poly(HNBMQ$_{1000}$-*r*-HNBMO$_{250}$) was 3.2×10^{-3} and 7.9×10^{-3} g dL^{-1}, respectively. The results indicate that the increase in the ratio of hydrophilic ammonium salt/hydrophobic ester-linkage alkyl chain increases the concentration of onset of micelle formation, which is due to hydrophobic association.

The values of I_3/I_1 in ethanol/methylene chloride [2/1 (v/v)] cosolvent are around 0.97 at lower polymer concentration (Fig. 6B), which is higher than in water due to the lower polarity of cosolvent. The CAC values of random poly(HNBMQ$_{500}$-*r*-HNBMO$_{250}$) and random poly(HNBMQ$_{750}$-*r*-HNBMO$_{250}$) in cosolvent are higher than in water, indicating that aggregation of unimers is easier in water than in cosolvent. However, random poly(HNBMQ$_{1000}$-*r*-HNBMO$_{250}$), which is hydrophobically cross-linked chains has lower CAC in cosolvent than in water. This result indicates the micropolarity related with the morphology of polymer aggregation.

The aggregates of the intra- and inter-polymer, consisting of hydrophobic microdomains surrounded by charged segments, may be viewed as polymer micelles, such as unimers or unicore multipolymer micelles. The formation of the polymer micelles may occur at a certain critical polymer

concentration, which is defined as a critical micelle concentration (CMC) for micelle-forming polymers [21]. When f_{HNBMQ} is increased from 67 to 75 mol%, all polymers in water exist as self-assembly unimeric micelles. The results of TEM and fluorescence spectroscopy on the micelles of different random copolymers containing various contents of ammonium salt in aqueous are summarized in Table 1. For the polymers in cosolvent, CMCs are not observed even at high concentration.

When f_{HNBMQ} is further increased to 80 mol%, polymer chains form much larger aggregates, which are different from that of the copolymer with f_{HNBMQ} less than 75 mol%. The structure of aggregates changed from spheres to network-like aggregates due to hydrophobically cross-linked chains. In this case, no critical micelle concentration was observed (Table 1 and Fig. 6A). Unfortunately, random poly($HNBMQ_{250}$-*r*-$HNBMO_{250}$) with $f_{HNBMQ(th)} = 50$ mol% ($f_{HNBMQ(exp)} = 48.7$ mol%) was soluble in ethanol and only partially soluble in water and methanol; hence, CMC could not be measured in aqueous solution.

The fluorescence spectral data of random and block copolymers with the same $f_{HNBMQ(th)}$ (91 mol%) at various concentrations are presented in Fig. 7.

The block copolymer (poly($HNBMQ_{1000}$-*b*-$HNBMO_{100}$) exhibited lower critical aggregation concentration ($CAC = 2.5 \times 10^{-4}$ g dL^{-1}) than that of the random copolymer (poly($HNBMQ_{1000}$-*r*-$HNBMO_{100}$) ($CAC = 5.0 \times 10^{-2}$ g dL^{-1}). Furthermore, it can be seen that the block copolymer exhibited a well defined CMC at a concentration of 4.0×10^{-2} g dL^{-1}, while CMC was not observed for the random copolymer even at high concentration (3.2 g dL^{-1}). This study clearly demonstrates that the block copolymer [block poly($HNBMQ_{1000}$-*b*-$HNBMO_{100}$)] with block hydrophobic and hydrophilic segments has much tendency to undergo association and to form micelles than corresponding random copolymer [random poly($HNBMQ_{1000}$-*r*-$HNBMO_{100}$)].

Fig. 8 displays emission spectra of the cationic random poly($HNBMQ_{500}$-*r*-$HNBMO_{250}$) ($f_{HNBMQ(exp)} = 67.2$ mol%) at different polymer concentrations of 5.6×10^{-4} [CAC, Fig. 8A], 5.7×10^{-1} [higher than CAC, Fig. 8B] and 0.1 g dL^{-1} [CMC, Fig. 8C] of pyrene molecules in the presence and absence of the polymers in aqueous solution. Monomer emission of pyrene could be observed in the range from 377 to 385 nm and the excimer emission could be observed in the range from 450 to 480 nm. The peak maximum at 377 nm arises from the fluorescence emission of isolated pyrenes (monomer emission). The broad band centered around 450 nm results from emission of excited dimeric pyrene (excimer emission).

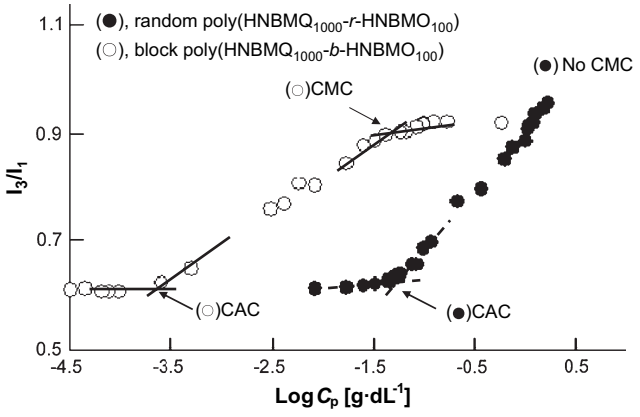

Fig. 7. Plots of log C_p *vs.* I_3/I_1 ratio for random copolymers, poly($HNBMQ_{1000}$-*r*-$HNBMO_{100}$) (●) and block copolymer, poly($HNBMQ_{1000}$-*b*-$HNBMO_{100}$) (○) in aqueous.

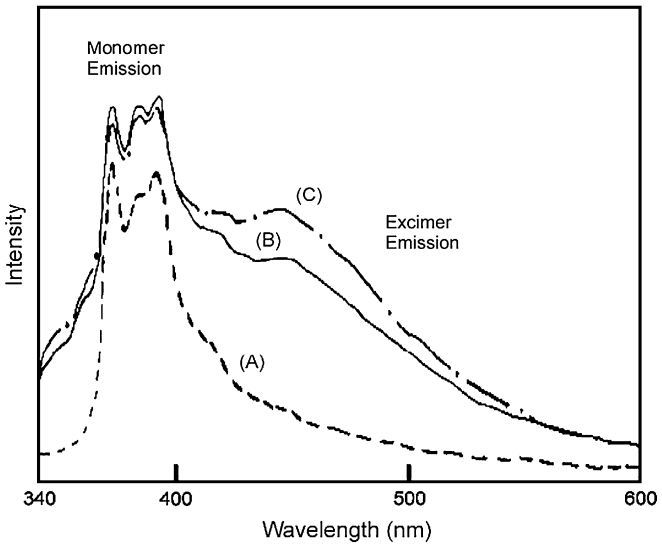

Fig. 8. Emission spectra of pyrene at different concentrations of random poly($HNBMQ_{500}$-*r*-$HNBMO_{250}$) in aqueous solution. (A) 5.6×10^{-4} (CAC), (B) 5.7×10^{-1} (between CAC and CMC) and (C) 0.1 g dL^{-1} (CMC).

Fig. 9 plots I_E/I_M as a function of polymer concentration in water (Fig. 9A) and in ethanol/methylene chloride cosolvent [ethanol/methylene chloride = 2/1 (v/v)] (Fig. 9B). The association of pyrene hardly exists, and I_E/I_M almost keeps unchanged when the polymers are at low concentrations. As the polymer concentration increases, the degree of excimer formation increases the population of excited pyrene dimers, which results in I_E/I_M increase [19]. For the aqueous system shown in Fig. 9A, the I_E/I_M curves depend on the composition of polymers. The I_E/I_M increases rapidly at 0.01 g dL^{-1} ($\log C_p = -2.0$) for poly($HNBMQ_{500}$-*r*-$HNBMQ_{250}$) and 0.2 g dL^{-1} ($\log C_p = -0.7$) for poly($HNBMQ_{750}$-*r*-$HNBMQ_{250}$). For the hydrophilic contents lower than 80 mol%, the excimer formation is at higher concentration for the polymer with higher hydrophilic content. While the I_E/I_M value increases rapidly at 0.016 g dL^{-1} ($\log C_p = -1.8$) for poly($HNBMQ_{1000}$-*r*-$HNBMO_{250}$), which is lower than that of poly($HNBMQ_{750}$-*r*-$HNBMQ_{250}$). This variation might result from the different morphologies of polymer micelles. These results are in agreement with the conceptual illustration of self-assembly micelles (Fig. 5). For the cosolvent system as shown in Fig. 9B, the I_E/I_M curves of the random polymers are almost the same. The random copolymers begin to associate, and as a result, the I_E/I_M value increases rapidly at 0.1 g dL^{-1} ($\log C_p = -1$), indicating that strong association occurs. Pyrene molecules are hydrophobic and easier to be embraced in

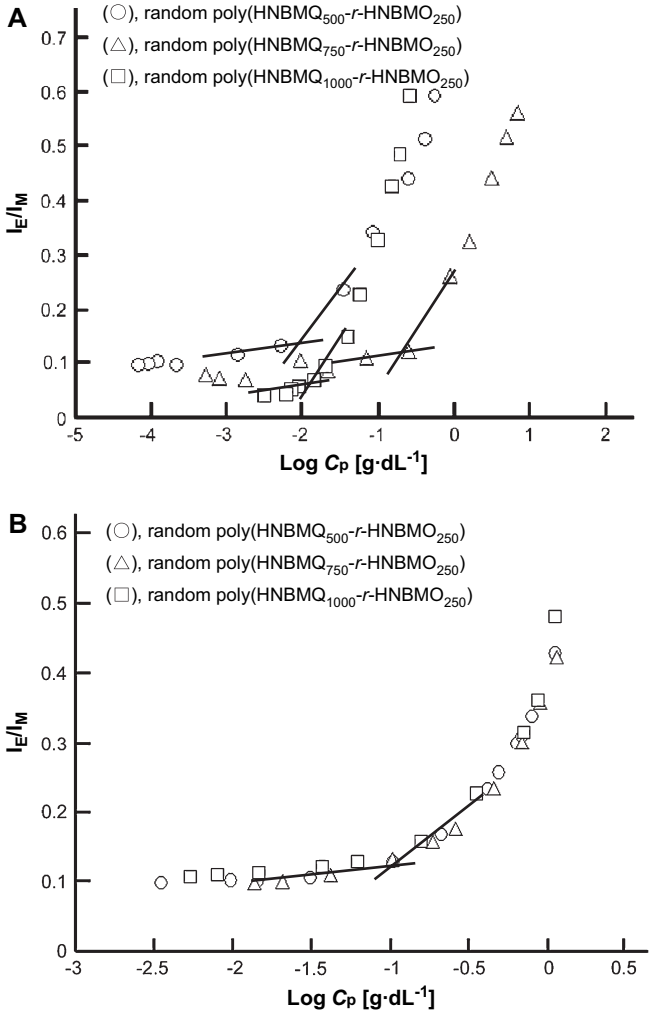

Fig. 9. Excimer emission/monomer emission (I_E/I_M) of random poly(HNBMQ-*r*-HNBMO)s in (A) water and (B) cosolvent [ethanol/methylene chloride = 2/1 (v/v)]. I_M: fluorescence intensity at 330 nm; I_E: fluorescence intensity at 450 nm. The content of ammonium = 67 mol% (○), 75 mol% (△), and 80 mol% (□).

hydrophobic association in aqueous. However, pyrene molecules are homogeneously distributed in the cosolvent. Therefore, less fluorescence information of pyrene for the formation of micelles in the cosolvent than in aqueous was observed. These results indicate that pyrene is a better fluorescence probe for the characterization of polymer assemblies in aqueous than in the cosolvent.

4. Conclusion

A series of novel polynorbornene copolymers with self-assembly amphiphilic architecture containing hydrophilic ammonium salt and hydrophobic alkyl ester group were obtained via ring-opening metathesis polymerization (ROMP). Spherical micelles of such polynorbornenes are formed in an ethanol/methylene chloride (2/1) solution by varying the content of ammonium salts from 50 to 75 mol% of random copolymers. When the hydrophilic content of the random copolymer is higher than 80 mol%, the morphology of micelles transferred into network-like aggregates. Block copolymer has much tendency to undergo association and form micelles than the corresponding random copolymer. The topology of such amphiphilic copolymers having highly stable polynorbornene main chains makes them attractive for nanomaterial applications.

Acknowledgements

The authors would like to thank the financial support of National Science Council (NSC) of Republic of China.

References

[1] Guyot A, Tauer K. Adv Polym Sci 1994;43:111.
[2] Torchilin V, Trubetskoy V. Adv Drug Delivery Rev 1995;16:141.
[3] Torchilin V. J Controlled Release 2001;73:137.
[4] Nishikawa M, Takakura Y, Hashida M. Adv Drug Delivery Rev 1996; 21:135.
[5] Takakura Y, Mahato R, Nishikawa M, Hashida M. Adv Drug Delivery Rev 1996;19:377.
[6] Hodoshima N, Udagawa C, Ando T, Fukuyasu H, Watanabe H, Nakabayashi S. Int J Pharm 1997;146:81.
[7] Junping W, Takayama K, Nagai T, Maitani Y. Int J Pharm 2003;251:13.
[8] (a) Cen L, Neoh KG, Kang ET. Langmuir 2003;19:10295;
(b) Chen CZ, Cooper SL. Biomaterials 2002;23:3359;
(c) Kim JY, Lee JK, Lee TS, Park WH. Int J Biol Macromol 2003;32:23;
(d) Chen JC, Yeh JT, Chen CC. J Appl Polym Sci 2003;90:1662;
(e) McCubbin PJ, Forbes E, Gow MM, Gorham SD. J Appl Polym Sci 2006;100:538;
(f) Sauvet G, Fortuniak W, Kazmierski K, Chojnowski J. J Polym Sci Polym Chem Ed 2003;41:2939;
(g) Kenawy ER, Mhamoud YA. Macromol Biosci 2003;3:107.
[9] Wan MW, Yen TF. Appl Catal A Gen 2007;319:237.
[10] Kim JJ, Shin DH, Lee HS, Park DW. Polym Adv Technol 2003;14:521.
[11] Ikeda T, Tazuke S, Suzuki Y. Makromol Chem 1984;185:869.
[12] Liaw DJ, Tsai JS, Wu PL. Macromolecules 2000;33:6925.
[13] Liaw DJ, Chen TP, Huang CC. J Polym Sci Polym Chem Ed 2005; 43:4233.
[14] Liaw DJ, Tsai JS, Sang HC. J Polym Sci Polym Chem Ed 1998;36:1785.
[15] Liaw DJ, Tsai CH. J Mol Catal A 1999;147:23.
[16] Liaw DJ, Chen TP, Huang CC. Macromolecules 2005;38:3533.
[17] Liaw DJ, Huang CC. J Polym Sci Polym Phys Ed 1998;36:11.
[18] Kalyanasundaram K, Thomas JK. J Am Chem Soc 1977;99:2039.
[19] Kramer MC, Steger JR, McCormick CL. Proc Am Chem Soc Div Polym Mater Sci Eng 1994;71:413.
[20] Noda T, Hashidzume A, Morishima Y. Macromolecules 2000;33:3694.
[21] Kramer MC, Welch CG, Steger JR, McCormick CL. Macromolecules 1995;28:5248.